IRIS AperTO

UNIVERSITÀ DEGLI STUDI DI TORINO

AperTO - Archivio Istituzionale Open Access dell'Università di Torino

Crystallization Behavior of Fe50−xCr15Mo14C15B6Mx (x = 0, 2 and M=Y, Gd) Bulk Metallic Glasses and Ribbons by in situ High Temperature X-Ray Diffraction

This is the author's manuscript

Original Citation:

Availability:

This version is available http://hdl.handle.net/2318/130424 since 2016-08-20T17:13:16Z

Published version:

DOI:10.1088/0256-307X/29/10/108103

Terms of use:

Open Access

Anyone can freely access the full text of works made available as "Open Access". Works made available under a Creative Commons license can be used according to the terms and conditions of said license. Use of all other works requires consent of the right holder (author or publisher) if not exempted from copyright protection by the applicable law.

(Article begins on next page)

25 April 2024

IRIS AperTO

UNIVERSITÀ DEGLI STUDI DI TORINO

This is the author's final version of the contribution published as:

Badis Bendjemil; Abderrezak Bouchareb; Ahmed Belbah; Jamel Bougdira; Rafael Piccin; Marcello Baricco. Crystallization Behavior of Fe50–xCr15Mo14C15B6Mx (x = 0, 2 and M=Y, Gd) Bulk Metallic Glasses and Ribbons by in situ High Temperature X-Ray Diffraction. CHINESE PHYSICS LETTERS. 29 pp: 108103-1-108103-4.
DOI: 10.1088/0256-307X/29/10/108103

The publisher's version is available at:
http://stacks.iop.org/0256-307X/29/i=10/a=108103?key=crossref.2723464eb47317ec6bc1319957f1c69f

When citing, please refer to the published version.

Link to this full text:
http://hdl.handle.net/2318/130424

This full text was downloaded from iris - AperTO: https://iris.unito.it/

iris - AperTO

University of Turin's Institutional Research Information System and Open Access Institutional Repository

Crystallization Behavior of $Fe_{50-}Cr_{15}Mo_{14}C_{15}B_6M$ (= 0, 2 and M = Y, Gd) Bulk Metallic Glasses and Ribbons by in situ High Temperature X-Ray Diffraction

Badis Bendjemil[1,2**], Abderrezak Bouchareb[1], Ahmed Belbah[2],
Jamel Bougdira[3], Rafael Piccin[4], Marcello Baricco[4]
[1]LEREC, Department of Physics, University of Badji-mokhtar-Annaba, Algeria
[2]Department of Mechanical Engineering, Faculty of Science and Technology, University of 8 Mai 1945 Guelma, Algeria [3]Institut Jean LAMOUR, University Henri poincarré, Nancy, France
[4]IFM/NIS, Università di Torino, Via P. Giuria 9, 10125 Torino, Italy

Abstract
The effect of rare earth addition on thermal stability of $Fe_{50-}Cr_{15}Mo_{14}C_{15}B_6M$ (= **0**, 2 and M=Y, Gd) is stud-ied. Thermal and structural properties are measured using differential scanning calorimetry and x-ray diffraction, respectively. The microstructure is observed by using a scanning electron microscope, and chemical composition is checked by energy dispersive spectroscopy analysis. The effect of high temperature on the isothermal crystalliza-tion of $Fe_{50-}Cr_{15}Mo_{14}C_{15}B_6M$ (= **0**, 2 and M=Y, Gd) bulk metallic glass and ribbons is investigated by high-temperature x-ray diffraction. It is found that the crystallization behavior of $Fe_{50-}Cr_{15}Mo_{14}C_{15}B_6M$ (= **0**, 2 and M=Y, Gd) bulk metallic glass strongly depends on the annealing temperature. The different crystallization behavior is believed to be due to the different structures that the metallic glass possesses at different temperatures.

Iron based amorphous alloys are considered to be promising candidates for many industrial appli-cations because of their unique properties, such as high strength and hardness, ultra-soft magnetic and high corrosion resistance.[1,2] Since 1995 many Fe-based bulk metallic glasses (BMGs) with high glass formability (GFA) have been published.[3–6] Investigation of the crystallization behavior of Fe-based BMGs has recently received considerable attention due to the importance of assessing its structural condition and establishing its thermal stability for possible applications.[7] Crystallization studies of metallic glasses are interesting from many points of view. The results of such studies are helpful in understanding the mechanism and kinetics of phase transformation into the equilibrium state. They also allow us to evaluate the glass forming ability from the melt and predict stability of the amorphous state. Moreover, the crystallization studies make a controlled production of micro-and nanostructures possible. Amorphous alloys are thermodynamically metastable. On increase of temperature, such non-crystalline systems transform into a crystalline state in the course of time. Usually, the crystallization event of a metallic glass upon heating may be studied experimentally using isothermal or non-isothermal analysis techniques. In the present study, crystallization kinetics have been presented as a function of annealing temperature of bulk metallic glasses $Fe_{50}Cr_{15}Mo_{14}C_{15}B_6$ with and without Gd and Y addition. The isothermal crystallization is investigated by in situ high temperature x-ray diffraction. The results of the onset and offset temperature of crystallization are compared to crystallization curves of differential scanning calorimetry (DSC).

Ingots of $Fe_{50-}Cr_{15}Mo_{14}C_{15}B_6M$ (M = Y, Gd and = 0, 2) master alloys were prepared from commercial-grade materials ~~using an arc-melting furnace under Ar atmosph~~ere. In order to study the effect of the Y and Gd on GFA, the liquid alloys were quenched in a copper mold. Bulk sample preparation was performed in a commercial casting machine used for the jewellery industry. It consists of an up-per chamber, in which the induction coil and the crucible are placed, and a lower one, which contains the copper mold. Both chambers can be evacuated un-til 10^{-1} mbar and subsequently filled with pure Ar. For comparison, ribbons of 5 mm width and about 30 m thickness were prepared using a single-roller melt spinner at a wheel speed of 24 m/s. High temperature x-ray diffraction (HT-XRD) was performed to examine the evaluation of the structure of the samples using a Panalytical X'Pert pro MPD diffractometer equipped with a high temperature chamber HTK 1200 under Ar atmosphere, using the Cu K radiations (= 1.5418 Å). Samples were placed inside a furnace which contains a hole through which the x-rays transmit, in situ HT-XRD measurements were continuously heated from ambient temperature to the measurement temperature. Then, the sample was held isothermally at this temperature for about 5 min and in the meantime the in situ HT-XRD measurement was performed, this operation was continuously repeated for the same sample until 1000°C, at a constant heating rate; it was estimated at 10°C/min. The average crystal sizes were estimated using the Scherrer equation.[8] The phases were identified using the soft-ware PCPDFWIN (International Centre for Diffraction Data, USA, 1997), scanning electron microscopy (SEM) investigations of the surface of the samples were performed using a Leica Stereoscan 420 micro-scope. The chemical compositions were checked using energy dispersion spectroscopy (EDS). Thermal analysis was performed by a Setaram high temperature differential scanning calorimeter (HT-DSC) at a heating rate of 10 C/min. The samples were placed in an alumina pan with some surrounding alumina pow-der, in order to prevent sticking to the crucible walls. The calorimetric cell was evacuated and purged several times before measuring under flowing He. Calibration of the instrument was performed from the temperature and heat of the fusion of pure metals (Al, Ag, Au, Fe, Cu, Ni).

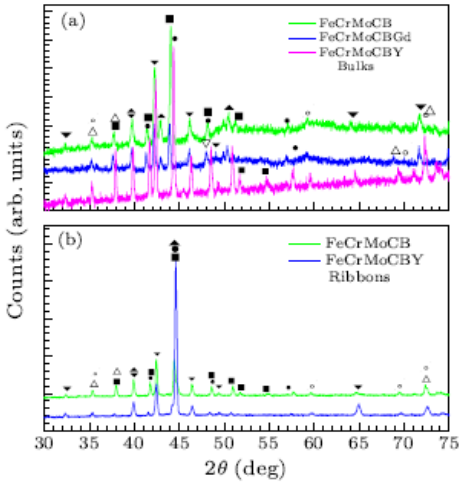

Fig. 1. XRD patterns of samples heated at 1000◦C and cooled at ambient temperature. Fe_3Mo_3C (inverted tri-angle), $Fe_{23}(C, B)_6$ (closed circle),$Cr_{23}C_6$ (square), Fe_3C (open circle), Cr_3C_2 (open triangle), $(Cr, Fe)_7C_3$ (closed triangle).

The as-cast structure and glass forming ability (GFA) of the $Fe_{50-}Cr_{15}Mo_{14}C_{15}B_6M$ (= 0, 2 and M=(Y, Gd) has already been studied and published in a previous work.[9] The XRD patterns of the samples $Fe_{50-}Cr_{15}Mo_{14}C_{15}B_6M$ (= 0, 2 and M=Y, Gd) bulk and ribbons revealed in Figs. 1(a) and 1(b), were heated at 1000◦C and rapidly cooled to ambient temperature, those patterns contain Bragg's peaks indicating that all of the samples were devitrified. The phases which appeared were $Fe_{23}(C, B)_6$, $Cr_{23}C_6$, Fe_3Mo_3C and $(Cr, Fe)_7C_3$. The average grain size of bulks with the compositions $Fe_{50}Cr_{15}Mo_{14}C_{15}B_6$, $Fe_{48}Cr_{15}Mo_{14}C_{15}B_6Gd_2$ and $Fe_{48}Cr_{15}Mo_{14}C_{15}B_6Y_2$ were estimated to be 20 nm, 11 nm and 40 nm, respectively, and ribbons with the compositions $Fe_{50}Cr_{15}Mo_{14}C_{15}B_6$ and $Fe_{48}Cr_{15}Mo_{14}C_{15}B_6Y_2$ were estimated as 11 nm and 34 nm respectively. During annealing, those samples underwent morphological change by the mechanisms of nucleation and growth, where the atoms became long range order due to thermal agitation. Figures 2(a), 2(b) and 2(c) show the XRD patterns of the bulk and ribbon samples which were treated from ambient temperature to 1000◦C. The bulk with the composition $Fe_{50}Cr_{15}Mo_{14}C_{15}B_6$ was partially crystallized be-fore thermal treatment, whereas the bulk and ribbon with the compositions $Fe_{48}Cr_{15}Mo_{14}C_{15}B_6Gd_2$ and $Fe_{50}Cr_{15}Mo_{14}C_{15}B_6$, respectively, were fully amorphous before thermal treatment. It is observed that the XRD patterns of the bulk with the composition $Fe_{50}Cr_{15}Mo_{14}C_{15}B_6$ reveal the evaluation of Bragg's peaks from ambient temperature until 700◦C, corresponding to partially crystallized, the fraction of crystallization increases until 800◦C, where the sample be-came fully crystallized. The phases which appeared are essentially $Fe_{23}(C, B)_6$, Fe_3Mo_3C, $(Cr, Fe)_7C_3$ and $Cr_{23}C_6$. The average grain size varies between 7 nm and 27 nm as shown in Fig. 4. In this case, the ab-sence of rare earth such as Gd/Y can facilitate atomic mobility which leads to a fully crystalline structure.

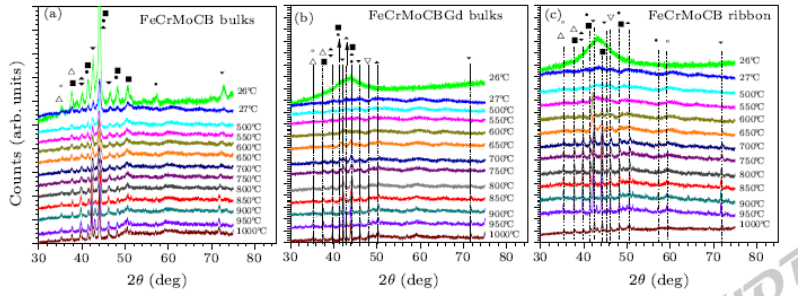

Fig. 2. XRD patterns as a function of annealing temperature showing the structure evolution and phases identified are Fe_3Mo_3C (inverted triangle), $Fe_{23}(C,B)_6$ (closed circle), $Cr_{23}C_6$ (square), Fe_3C (open circle), Cr_3C_2 (open triangle), and $(Cr, Fe)_7C_3$ (closed triangle).

On the other hand, the bulk sample with the composition $Fe_{48}Cr_{15}Mo_{14}C_{15}B_6Gd_2$ as shown in Fig. 2(b) exhibits broad diffraction maxima characteristic of an amorphous structure without apparent crystalline peaks until 650◦C; at this temperature some peaks appear and the sample becomes partially crystallized. Thereby, the crystallization fraction increases, which leads to completely crystalline structure at 900◦C, the identified phases are of $Fe_{23}(C, B)_6$, Fe_3Mo_3C, $(Cr, Fe)_7C_3$ and $Cr_{23}C_6$, the average particle sizes are estimated to be from 5 nm to 32 nm, as shown in Fig. 4. Moreover, ribbon with composition $Fe_{50}Cr_{15}Mo_{14}C_{15}B_6$, which is represented in Fig. 2(c), shows a large halo peak without sharp peaks corresponding to the fully amorphous material until 600◦C, at this temperature a broad halo peak superimposes

the sharp peak characteristics of crystalline phases, suggesting the presence of a mixture of amorphous and crystalline phases, which become fully crystallized at about 800◦C. The phases which appeared are essentially $Fe_{23}(C, B)_6$, Fe_3Mo_3C, $(Cr, Fe)_7C_3$ and $Cr_{23}C_6$ and average grain sizes are estimated to be from 7 nm to 22 nm as shown in Fig. 4.

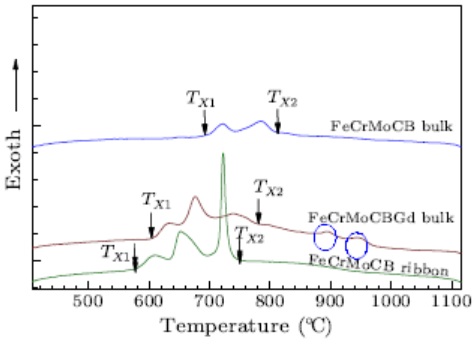

Fig. 3. DSC scan showing the onset and offset crystal-lization temperatures.

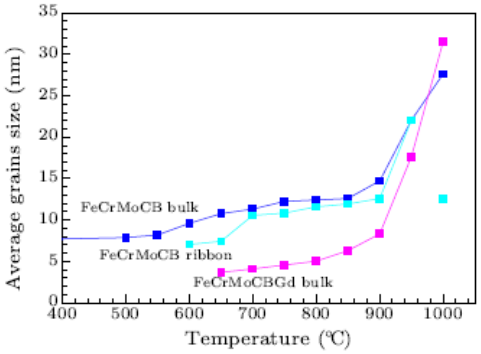

Fig. 4. Average grain size as a function of annealing tem-perature.

Figure 3 shows the DSC crystallization curves of the bulk samples with the compositions $Fe_{50}Cr_{15}Mo_{14}C_{15}B_6$, $Fe_{48}Cr_{15}Mo_{14}C_{15}B_6Gd_2$ and ribbon sample $Fe_{50}Cr_{15}Mo_{14}C_{15}B_6$. It can be observed that the DSC curve of the bulk with the composition $Fe_{50}Cr_{15}Mo_{14}C_{15}B_6$ exposes two exothermic events, which are limited by the onset and offset crystallization temperatures $_1$ = 694◦C and $_2$ = 815◦C respectively. The sample has a partially crystalline structure between $_1$ and $_2$. Thereby, this do-main demonstrates that the fraction transformed during thermal treatment from the amorphous phase is gradually increased, which leads to a fully crystalline structure at $_2$ = 815◦C. On the other hand, the DSC curve of the bulk sample with the composition $Fe_{48}Cr_{15}Mo_{14}C_{15}B_6Gd_2$ shows three evident exothermic peaks between $_1$=604◦C and $_2$ = 780◦C. Thus, the fraction transformed increases from $_1$ to $_2$ and the structure remains partially crystallized at $_2$ = 780◦C, because two small exothermic peaks, indicated by two circles in Fig. 4, are at the high temperatures 885◦C and 930◦C, suggesting two amorphous phases which are residual during thermal treatment. The nucleation and growth of particles are difficult in presence the rare earth (Gd) in the alloy. This leads to a fully crystalline structure at 930◦C. More-over, the DSC curve of the ribbon sample with the composition $Fe_{50}Cr_{15}Mo_{14}C_{15}B_6$ presents three crystallization peaks. They are limited by the onset and offset temperatures $_1$ = 579◦C and $_2$ = 745◦C, respectively. In this case, the fraction transformed increases by nucleation and growth mechanisms of crystallites, which lead to a fully crystallized structure at $_2$ = 745◦C.

Table 1 shows the values of the onset and offset crystallization temperatures of the bulks and ribbon, analyzed by HT-XRD and DSC. The values are similar to those of measurement techniques which make some error during annealing.

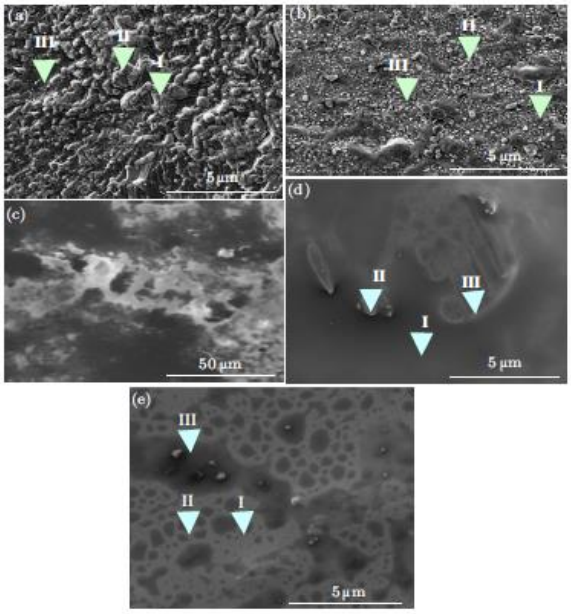

Fig. 5. SEM images of $Fe_{50-}Cr_{15}Mo_{14}C_{15}B_6M$ (= ***0***, 2 and = , Gd): (a) Fe_{50}, (b) Fe_{48}(Y), (c) Fe_{48}(Gd) and ribbons, (d) Fe_{50}, (e) Fe_{48}(Y).

However, it can be seen that the crystallization temperature values vary from one composition to an-other. The influence of a proper rare earth (Gd) substitution for Fe on thermal stability is clear when we compare the XRD patterns of the composition $Fe_{48}Cr_{15}Mo_{14}C_{15}B_6Gd_2$ BMG with the XRD pat-terns of the bulk and ribbon of the composition $Fe_{50}Cr_{15}Mo_{14}C_{15}B_6$. It can be seen that the bulk of the second composition is partially crystallized at ambient temperature.

Even so, the first composition is completely amorphous, suggesting that the addition of a suitable amount of Gd in the alloy is beneficial for making metallic glass. The large size of Gd atoms compared with other elements can also increase the pack density of the alloy, thereby bypassing the nucleation and growth of crystalline phases during heating. At a certain temperature the atoms of the alloy begin to move and the critical energy barrier is passed due to thermal agitation leading to the formation of crystalline phases which start from about 650°C according to the XRD patterns in Fig. 2(b).

Figure 4 present the average grain size as a function of annealing temperature. It can be seen that average grain size increases exponentially with annealing temperature for all of the samples. A rapid increase in size is noted at 900°C, provoked by the germination and growth of crystallites at high temperature.

Table 1. Onset and offset crystallization temperatures $_1$ and $_2$ of HT-XRD and DSC.

	$Fe_{50}Cr_{15}Mo_{14}C_{15}B_6$ Bulk		$Fe_{48}Cr_{15}Mo_{14}C_{15}B_6Gd_2$ Bulk		$Fe_{50}Cr_{15}Mo_{14}C_{15}B_6$ Ribbons	
	$_1$ (°C)	$_2$ (°C)	$_1$ (°C)	$_2$ (°C)	$_1$(°C)	$_2$ (°C)
HT XRD	700	800	650	900	600	800
DSC	694	815	604	930	579	745

The SEM microstructure images of the annealed samples are presented in order to identify the phases which appear at the end of heat treatments. The identified phases are determined from the EDS results and the estimated average atomic weight. Figure 5(a) shows the SEM image of the sample with the nominal composition $Fe_{50}Cr_{15}Mo_{14}C_{15}B$. This sample is partially amorphous before heat treatments. However, from the SEM picture, it can be seen that the sample is completely crystallized, the grains having different sizes and shapes, some of them are spherical, and these grains are generated from the nucleation and growth of dendrite phases due to the heat treatments. The SEM microstructure is composed of three regions and, from EDS analysis, shows that the dendrite phases are enriched in Mo by region I, corresponding to Fe_3Mo_3C surrounded by area II enriched in Cr, which is assigned to a mixture of two carbide phases $Fe_{23}(C, B)_6$ and $Cr_{23}C_6$ crystal structure. Small particles enriched in Cr are observed in area III, probably due to the nucleation and growth of crystals in car-bide phases corresponding to Fe_3C or Cr_3C_2 at various temperatures. On the other hand, the SEM im-age of the sample annealed with the nominal composition $Fe_{48}Cr_{15}Mo_{14}C_{15}B_6Y_2$ is fully amorphous (bulk metallic glasses, BMG) before heat treatments. At the end of heat treatments, the microstructure in Fig. 5(b) shows a complete crystallization of the sample. We can also see grains with various shapes and sizes, mostly small bright particles distributed along the sur-face. The microstructure may be composed of three regions. EDS analysis shows that phase I is enriched in Mo and Y assigned to Fe_3Mo_3C. Some grains with the same size and shape

occupy various places, most of them with a hexagonal shape are observed in phase II enriched in Cr confirming the formation of carbide phases $Fe_{23}(C, B)_6$ and $Cr_{23}C_6$. While phase III, com-posed of small particles, is enriched in Cr assigned to Fe_3C or Cr_3C_2. In addition, the microstructure of the annealed sample is fully amorphous (bulk metallic glasses, BMG) before heat treatment with the nominal composition $Fe_{48}Cr_{15}Mo_{14}C_{15}B_6Gd_2$, as shown in Fig. 5(c).

Two main phases are observed in the dark and white phases. From EDS analysis of enrichment in Mo and Gd, a bright phase is observed, confirming that the formation of Fe_3Mo_3C and enrichment in Cr is ob-served in the dark phases assigned to carbide phases.

It could not provide further information because the phases were so close to each other so that the relative contrast could not be achieved. It could also be related to the small size of the crystals. The rib-bon metallic glasses are also annealed at various temperatures. Figures 5(d) and 5(e) show the SEM microstructure of the samples with the nominal composition $Fe_{50}Cr_{15}Mo_{14}C_{15}B_6$ and $Fe_{48}Cr_{15}Mo_{14}C_{15}B_6Y_2$, which are amorphous before heat treatments. Therefore, three phases can be seen according to the SEM microstructure. The EDS analysis of the microstructure shows that an enrichment in Mo is observed in phase I and an enrichment in Cr is observed in phases II and III assigned to phases Fe_3Mo_3C, carbide phases $Fe_{23}(C, B)_6$, $Cr_{23}C$ and Fe_3C or Cr_3C_2, respectively. These results are in agreement with the XRD patterns.

In summary, we have investigated a series of bulk and ribbon metallic glasses with the different compositions of Fe_{50-} $Cr_{15}Mo_{14}C_{15}B_6M$ (= 0, 2 and M = Y, Gd) which were annealed at various temperatures by in situ high temperature and x-ray diffraction. It is seen that the evaluation of the structures of all of the samples gradually increase with temper-ature. On the other hand, onset and offset of crystallization temperatures, demonstrated by HT-XRD, are rather similar to those shown by DSC analysis. It is also found that the dominant phases of all alloys are of Fe_3Mo_3C, $Fe_{23}(C, B)_6$, $(Cr, Fe)_7C_3$ and $Cr_{23}C$ crystals. The average grain size varies from 5 nm to 32 nm.

Dipartimento di chimica, IFM/NIS, Università di Torino, Italy and Institut Jean LAMOUR, University Henri Poincarré, Nancy, France are acknowledged.

References

[1] Mizushima T, Makino A, Yoshida S and Inoue A 1999 J. Appl. Phys. 85 4418
[2] Jartych E, Pekala K, Jaskiewicz P, Latuch J, Pekala M and Grabski J 2002 J. Alloys Compd. 343 216
[3] Inoue A 2000 Acta Mater. 48 306
[4] Inoue A, Shen B L 2002 Mater. Trans. JIM 43 769
[5] Stoica M, Eckert J, Roth S, Zhang Z F, Schultz L and Wang W H 2005 Intermetallics 13 764
[6] Pang S J, Zhang T, Asami K and Inoue A 2002 Corros. Sci. 44 1847
[7] Baser T A and Baricco M 2008 J. Mater. Res. 23 2166
[8] Gloriant T, Gich M, Surinach S, Bar, M O and Greer A L 2000 Mater. Sci. Forum 343-346 365
[9] Bouchareb A, Bendjemil B, Piccin R and Baricco M 2010
Chin. Phys. Lett. 27 076103